



INCREASING PROPULSIVE FORCE IN JET ENGINE USING D-B INJECTORS

¹. Fathollah OMMI, ². Koros NEKOFAR, ¹. Ehsan MOVAHEDNEJAD

¹ Faculty of Engineering, Tarbiat Modares University, Tehran, IRAN
²Iranian Space Agency (ISA), Tehran, IRAN

ABSTRACT:

In this work the fundamentals of centrifugal injector's calculation are reviewed and new design procedure is proposed for liquid-liquid injectors, based on both theory and experimental results. Then some special conditions related to dual based liquid-liquid injectors are studied and the corresponding results were considered in design manipulation. The behavior of injector in various service conditions, such as mutual effects on twin spray envelopes in dual-base injector is investigated, and then the design procedure is presented based on obtained results. Finally the computer program for designing this sort of injector is proposed. Using this program, some injectors were designed and tested. The results were presented in details in this paper.

KEYWORDS:

Injector, Dual-base, Liquid-Liquid, Propulsion, jet

1. INTRODUCTION

The dual based liquid-liquid injectors have many advantages which have given them the capability of many applications in jet industries. Using these injectors, a very better mixing between fuel and oxidizer can be achieved, which causes better combustion conditions and reduction in probability of combustion instability. In addition, since the fuel and oxidizer are both exhausted from one injector, it is possible to have higher discharge rate of fuel and oxidizer without any increase in the diameter of injector plate and in the same way, obtain higher thrust or in case of having fixed discharge rate, it is possible to decrease combustion chamber diameter. This, in turn, gives higher pressure in the combustion chamber.

The centrifugal system is used in designing and manufacturing of liquid-liquid base injectors. One of the main advantages of these injectors is the capability of producing spray with desirable spray angle and forming Micro-diameter drops which provide perfect combustion.

In the presented design procedure, the governing equations for an ideal fluid are solved and the results are corrected using some correction factors based on experimental data. The rules used in the centrifugal injector theory are based on the principles of mass, angular momentum and energy conservation or Bernoulli's Equation and maximum flow rate and minimum energy laws that are explained below.

Fig.1 shows a schematic of a centrifugal injector in which d_{Bx} , L_{Bx} and D_K are the entrance whole diameter, the length of entrance hole and the rotation radius, respectively.

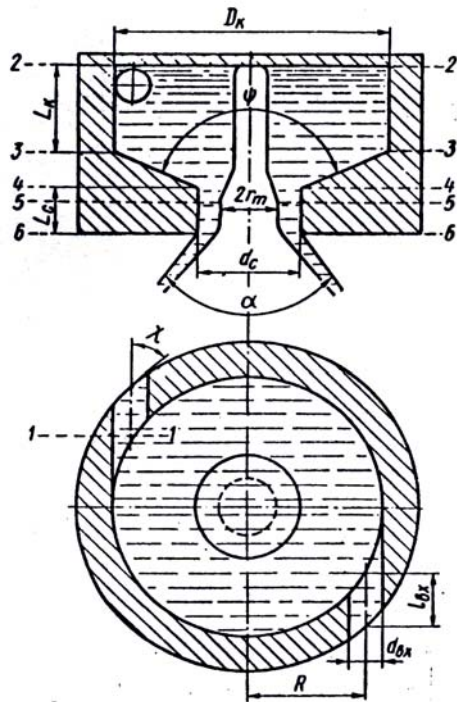


Fig.1 Centrifugal injector cross section [1]

The geometrical characteristic parameter of a centrifugal injector has an important rule in the design procedure and is defined as the following [1]:

$$A = \frac{Rr_c}{nr_c^2 BX} \quad (1)$$

where r_c is exit whole diameter of nozzle.

According to the conservation of angular momentum principle, parameter M is constant.

$$M = V_{ur} = V_{int}R = \text{const.} \quad (2)$$

The centrifugal force of the fluid increases as it passes through the injector. Due to this force, a hollow cylinder shape flow forms at the exit of the injector which is filled by air.

The cross section area of this flow is equal to:

$$FK = \pi(r_c^2 - r_m^2) = \varphi_c \pi r_c^2 \quad (3)$$

where r_m , r_c and φ_c are the inner, outer radius and nozzle contraction coefficient respectively.

φ_c is defined as:

$$\varphi_c = 1 - \frac{r_m^2}{r_c^2} \quad (4)$$

According the maximum mass flow rate principle, for an optimal amount of φ_c the discharge rate of the injector becomes maximum.

The injector flow rate is equal to:

$$G = \pi r_c^2 \mu \sqrt{2\rho \Delta p_\varphi} \quad (5)$$

In which, μ is called discharge rate coefficient which is a function of A and φ_c . Where, A is Geometrical characteristic. According to the explanations given above and the principal of maximum discharge rate, $d\mu/d\varphi_c = 0$ and from this, the relationship between A and φ_c is obtained.

2. THE FRICTION EFFECT ON THE FLOW

When the fluid passes through the entrance hole and reaches to swirl chamber, a pressure drop is formed in fluid (Δp_{BX}) that is equal to:

$$\Delta p_{BX} = \zeta_{BX} \frac{\rho V_{BX}^2}{2} \quad (6)$$

where ζ_{BX} , is the drop coefficient of entrance hole and is obtained from experimental tests. Fig.2 shows the variation diagram of ζ_{BX} as a function of Reynolds number (Re_{BX}) which is defined as the following:

$$Re_{BX} = \frac{V_{BX} d_{BX} \sqrt{n}}{\nu} \quad (7)$$

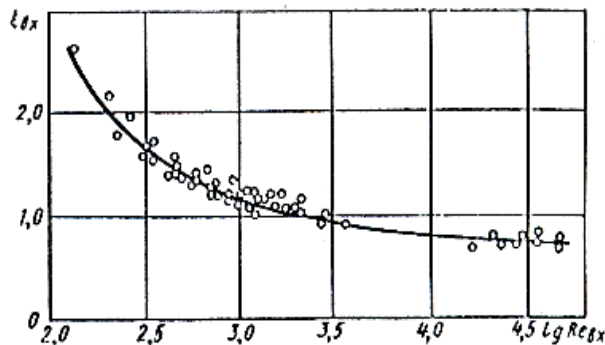


Fig.2 Diagram of the amount of input channel resistance ζ_{BX} and Reynolds number Re [1]

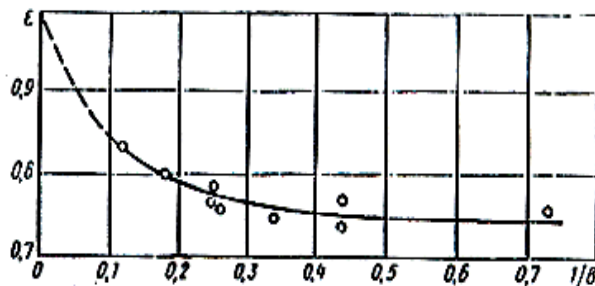


Fig.3 Relationship of amount of transformation input current ε and $1/B$

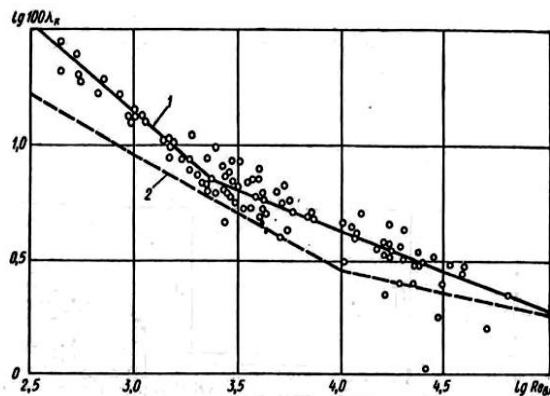


Fig. 4 Relationship between value of friction and the input Reynolds number [1]
1) Experimental relation, 2) Theoretical relations

When the fluid enters to swirl chamber from entrance hole, it contracts in a way that the average radius of rotation increases and changes from R to R_ε .

A coefficient named ε is defined here and is found from experimental tests as follows:

$$\varepsilon = \frac{R}{R_\varepsilon} \quad (8)$$

Fig.3 presents the variation of ε versus $1/B$, where $B = \frac{R}{r_{BX}}$.

Using the coefficient ε , the injector geometrical characteristic (A_D) can be calculated from:

$$A_D = \frac{Rr_c}{\varepsilon n r_{BX}^2} \quad (9)$$

There is a loss of energy inside the swirl chamber due to the friction between the fluid and the wall. The amount of friction is obtained using the friction coefficient λ_k which is obtained from fig.4.

The parameter θ is defined that shows the amount of the friction effects and is equal to:

$$\theta = \frac{\lambda_k}{2} A_D \left(\frac{R_k}{r_c} - 1 \right) \quad (10)$$

where R_k is the radius of swirl chamber.

A hydraulic jump occurs because of an abrupt change of flow path slope, just after the nozzle entrance cone. This in turns causes an energy loss in entrance channel (ΔBx) swirl chamber and the nozzle plays an important role in the design of injector.

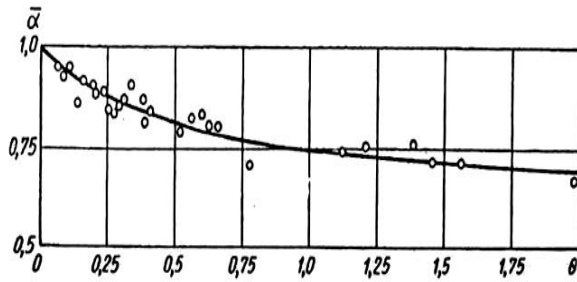


Fig. 5 Relationship of spray cone relative angle $\bar{\alpha}$ with θ set

The shape of spray is a cone with an angle of which its calculated value is corrected using the following correction factor:

$$\bar{\alpha} = \frac{\alpha_{EXP}}{\alpha_T} \quad (12)$$

Where α_{EXP} and α_T are experimental and theoretical values of α respectively.

Fig.5 shows the diagram of $\bar{\alpha}$ versus the θ collection.

3. CENTRIFUGAL INJECTOR DESIGN PROCEDURE

The centrifugal injector should provide the necessary discharge rate of the fluid under a definite spray cone angle and the pressure difference. It is also recommended to have minimum energy drop, in order to face with minimum reduce of exit flow velocity and injection quality.

As mentioned before the total amount of θ determines the effect of friction and the smaller value of θ show the smaller effects of fluid viscosity on the injector hydraulics.

For low viscosity liquids such as gasoline, oil and water, if the suitable rang of injector expansion coefficient ($C_c = \frac{R}{r_c}$) recommend within $1.25 \leq C_c \leq 5^\circ$. In this state as spray cone angle is larger; the size of C_c should be smaller. As the length of nozzle is not desirable, since it leads to a decrease in the spray cone angle, it is recommended to take ($\bar{L}_c = L_c/d_c$) in the range of $0.25 \leq \bar{L}_c \leq 1.0$. It is also recommended to take the input cone angle to nozzle (ψ) in the range of $60 \leq \psi \leq 120$ range. If the entry canals do not have sufficient length, the current fails in taking tangent direction and inclines towards the rotation chamber axis and as a result, the cone spray angle becomes smaller and the discharge coefficient becomes bigger. Therefore, the length of input canals should not be smaller than one and a half time of its internal diameter. On the other hand, this length should not be too large since in such situation, the energy loss resulted from friction becomes high.

In most injectors, 2 to 3 canals will be sufficient to make the symmetric spray cone becomes same with diffusion. When the number of canals becomes more than 3, no considerable change is made in the quality of fuel distribution; however, the injector structure becomes more complex and its precision becomes less. In open injectors (low amounts of C_c) the loss of energy reveals itself in input canals; thus, it is necessary to take C_c bigger than 1.25 ($C_c \geq 1.25$).

The hydraulic design of a simple centrifugal injector includes determining dimensions of nozzle, swirl chamber and input canals. The initial data consists of: the cone angle of spray, discharge rate, pressure difference of injector, and the entrance angle to nozzle, number of holes to the swirl chamber, density and fluid viscosity.

The design stages could be described:

1. Determine the values of ψ , n , C_c , V , ρ , G (Injector flow rate) Δp_ϕ and α .

2. Considering $\alpha_0 = 0.85$ as the first approximation from its range of variation, $0.5 \leq \alpha \leq 1$. and calculating the spray con angle from:

$$\alpha_1 = \frac{\alpha_0}{0.85} \quad (13)$$

3. Obtaining the value of A_{D1} using Fig.6 and the value of α_1 .

4. Determine the value of μ_1 using Fig.6.

5. Obtain the injector nozzle diameter from the following equation [3]:

$$d_{cl} = \sqrt{\frac{4G}{\pi\mu_1\sqrt{2P\Delta x_0}}} \quad (14)$$

6. Determine the swirl radius R_l , using chosen value of C_c and R_{cl} (Injector nozzle radius):

$$R_l = C_c R_{cl} \quad (15)$$

7. Calculating the entrance channel diameter using the following relation:

$$d_{BXL} = 2\sqrt{\frac{R_l r_{cl}}{\varepsilon_0 n A_{DI}}} \quad (16)$$

$\varepsilon_0 = 0.8$ as the first approximation.

8. Calculating the flow Reynolds number [4]:

$$Re_{BX1} = \frac{4G}{\rho v \pi d_{BX1} \sqrt{n}} \quad (17)$$

9. Determine the friction coefficient using Fig.4.

10. Calculate the injector equivalent characteristic length using [5]:

$$A_{cl} = \frac{A_{DL}}{1 + \theta_1} \quad (18)$$

where $\theta_1 = 0.5\sigma\lambda_{k1}A_{DL}(C_{k1} - 1)$ and $C_{k1} = C_c + \frac{r_{BX1}}{r_{cl}}$, $\sigma = \frac{1}{A_D} + \frac{\lambda_K}{2}C_k$ where σ surface tension.

11. Determine $\mu_{\theta 1}$ and $a_{\theta 1}$ using Fig.6.

12. Obtaining the value of α_1 using Fig.5.

13. Calculate the first approximation of spray cone angle [6].

$$\alpha_{p1} = \alpha_1 \alpha_{\theta} \quad (19)$$

14. Calculate the total energy loss in injector using Fig.2:

$$\Delta\Sigma\Delta B_{X1} + \Delta k_1 + \Delta C_1 \quad (20)$$

15. Calculating ΔB_{X1} using the following equation:

$$\Delta B_{X1} = \zeta_{BX} \frac{A^2}{C_c^2}, C_c = \frac{R}{r_c} \quad (21)$$

16. Calculating ΔK by the following equation [7]:

$$\Delta K = \frac{\lambda_k}{\sigma^2} \left\{ \frac{1}{\sigma} \left(1 - \frac{1}{C_k} \right) + \lambda_k \left[\frac{A_D}{2} - \frac{1}{2\sigma - \lambda_k} \left(\frac{2}{\sigma} + \frac{A_D}{2} + \frac{1}{2\omega - \lambda_K} \right) + \frac{3}{2\sigma^2} \ln \frac{(2\sigma - \lambda_k) A_D C_k}{2} \right] \right\} \quad (22)$$

$$\sigma = \frac{1}{A_D} + \frac{\lambda_K}{2} C_k \quad C_k = \frac{R_k}{r_c}$$

17. Selecting an appropriate value for nozzle resistance coefficient (ζ_c) in the range of 0.11 and 0.16 [1].

18. Obtaining φ_c using Fig.6 and considering $A = A_{cl}$.

19. Calculating ΔC_1 using the following equation:

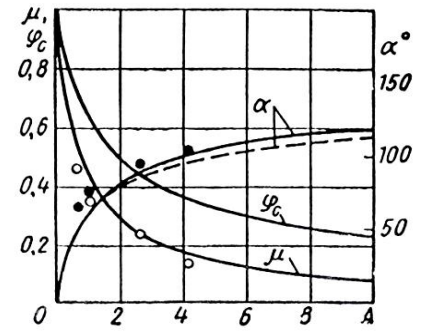


Fig.6 Relationship of discharge coefficient and nozzle contraction coefficient and spray cone angle to the geometric characteristic of injector [2]

$$\Delta c = \frac{\zeta_c}{\varphi_c^2} \quad (23)$$

20. Obtaining a first approximate value for μ_{p1} [8]:

$$\mu_{p1} = \frac{\mu_{\theta 1}}{\sqrt{1 + \Delta \Sigma_1 \mu_{\theta 1}^2}} \quad (24)$$

21. Calculating the coefficient of transformation, ε_1 , via Fig.3.

22. Updating the values of ε_1 , μ_{p1} and a_1 by comparing the calculated values of ε_0 , μ_1 and a_0 , where a_0 is spray angle of oxidizer. If the difference exceeds the permitted quantity, the second approximation is obtained. In this case, with respect to the given amount, the spray cone angle a_0 and amount of a_1 obtained from the first approximation is obtained to be as $a_0 = a_0 / a_1$.

23. Considering the value of a_2 and using Fig.6 the values of μ_2 and A_{D2} are calculated.

24. Calculating μ_2 using the obtained coefficient of energy loss (μ'_2), by the following expression.

$$\mu'_2 = \frac{\mu_2}{\sqrt{1 + \Delta \Sigma_1 \mu_2^2}} \quad (25)$$

25. Calculating the nozzle injector diameter using the following formula:

$$d_{c2} = \sqrt{\frac{4G}{\pi \mu'_2 \sqrt{2\rho \Delta p \Phi}}} \quad (26)$$

26. Obtaining the swirl radius by: $R_2 = C_c r_c$

27. Calculating the inlet channel diameter using the following expression [9]:

$$d_{Bx2} = 2 \sqrt{\frac{R_2 r_{c2}}{\varepsilon_1 n A_{D2}} - \frac{\lambda_{k1}}{2} \frac{R_2 r_{c2}}{\varepsilon_{in}} (C_{k1} - 1)} \quad (28)$$

Where, n is determined before and the amount of λ_{k1} , C_{k1} and ε_1 will obtain in the first approximation.

28. Reynolds number is calculated [10]:

$$Re_{BX2} = \frac{4G}{\rho v \pi d_{BX2} \sqrt{n}} \quad (29)$$

29. The friction coefficient is determined using Fig.5.

30. Obtaining the injector equivalent characteristic using:

$$A_{e2} = \frac{R_2 r_{c2}}{\varepsilon_1 n r_{BX2}^2 (1 + \theta_2)} \quad (30)$$

Where, $C_{k2} = C_c + \frac{r_{BX2}}{r_{c2}}$ and $\theta_2 = \frac{\lambda_{k2}}{2} \frac{R_2 r_{c2}}{\varepsilon_1 n r_{BX2}^2}$.

31. Determining the amounts of $\mu_{\theta 2}$ and $a_{\theta 2}$ using Fig.6.

32. Obtaining the value of a_2 by using Fig.5.

33. By using formula $\alpha_{p2} = \bar{\alpha}_2 \alpha_{\theta 2}$, the magnitude of the spray cone in second approximation is obtained.

34. Calculating the energy loss coefficient using the same procedure in the first stage.

35. The discharge coefficient in second approximation is obtained from following relations:

$$\mu_{p2} = \frac{\mu_{\theta 2}}{\sqrt{1 + \Delta \Sigma_2 \mu_{\theta 2}^2}} \quad (31)$$

36. Obtaining the value of ε_2 using the values of B_2 and ε_1 (Fig.3).

37. Comparing the calculated values of ε_2 , α_{p2} and μ_{p2} with the previous values of ε_1 , α_0 and μ_{p1} in order to calculate their approximation. If a good convergence can not be obtained, one has to select a smaller value for c_c and repeat the appropriate stages.

38. After calculation of d_c , R and d_{Bx} , other geometrical sizes of injector are calculated. The diameter of swirl enclosure is obtained in the next step by using this formula [11]:

$$D_k = 2(R + r_{Bx})$$

Then the nozzle length (L_c), inlet channel length (L_{Bx}) and swirl enclosure length (L_k) are selected, considering the aforementioned comments.

39. The proposed procedure has an extensive application and its results are precise within $\pm 10\%$.

4. THE DOUBLE-BASE CENTRIFUGAL INJECTOR CALCULATION

Fig.7 shows a Double-base injector [12]. In this injector, fuel and oxidizer are mixed outside the injector. The injector parameters should be selected in a way that the fuel and oxidizer spray cones do not cut each other near nozzle outlet. α_f and α_o show the spray angle of fuel and the angle of oxidizer, respectively. The design procedure of single injectors is applied for designing the double-base injector. An important point in designing this type of injector is that the gas vortex radius of the outer injector should be more than external radius of central injector nozzle. One should also consider that for the contact of two spray umbrella, the spray cone angle in the inner injector should be more than outer one.

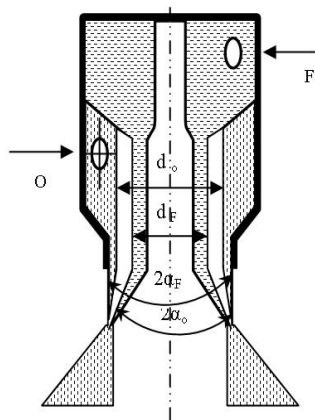


Fig.7 Dual-base external mixing injector [2]

in which $\bar{r}_{Bx} = r_{Bx0} \sqrt{\frac{K_m + 1}{K_m}}$. Considering the law of angular momentum conservation one may write [14]:

$$M = RV_{Bx} = \bar{R}V_{Bx0} \quad (35)$$

$$R_F = R_0 \gamma_R = R \gamma_R \quad \bar{R} = R \frac{(K_m + \gamma_R \sqrt{\frac{\rho_0}{\rho_F}})}{K_m + 1} \quad (36)$$

$$V_{Bx} = V_{Bx0} \frac{(K_m + \gamma_R \sqrt{\frac{\rho_0}{\rho_F}})}{K_m + 1} \quad (37)$$

According to the aforementioned relations, the geometric characteristic of a double-based centrifugal injector could be written as:

$$\bar{A} = \frac{K_m(K_m + \gamma_R \sqrt{\frac{\rho_0}{\rho_F}})}{(K_m + 1)(K_m + \frac{\rho_0}{\rho_F})} n_0 r_{Bx0}^2 \quad (38)$$

Expression for μ_ϕ , ϕ and a , are the same as those for single-base injector with substitution of \bar{A} by A . Therefore, one may write:

$$m_\phi = \mu_\phi F_{c\phi} \sqrt{2\rho_r \Delta P_\phi} \quad (39)$$

in which $\rho_T = \frac{\rho_0 \rho (1 + K_m)}{\rho_0 + K_m \rho_F}$ and μ_ϕ is the passage efficiency or total discharge rate coefficient and $F_{c\phi}$ is the cross section area of flux in nozzle.

Depending on the value of $C_c = \frac{R}{r_c}$, some corrections in discharge coefficient might be

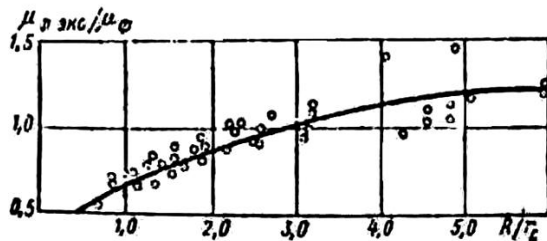


Fig.8 Correction factor of coefficient flow versus swirl radius

necessary. The relationship between experimental and theoretical discharge rate coefficient (μ_ϕ & $\mu_{\phi EXP}$) as a function of $\frac{R}{r_c}$ is presented graphically in Fig.8 [15].

5. RESULTS OF DESIGNING A DOUBLE-BASE INJECTOR

Based on the presented design procedure, a computer code is developed, which performs the design and necessary calculations of different dimensions of injector. This program designs injector based on design data and calculates its dimensions.

To design a double-base injector, the data of internal and external injector should be input in the program separately to obtain its geometry.

However, as mentioned, the radius of air vortex in the external injector should be more than the external radius of nozzle in the inner injector. At the same time, the spray cone angle of inner injector should be more than outer injector therefore both spray cones would contact after discharging from injector. Fig.9 and 10 present the results and comparison between the experimental and calculated values for a specific set of design conditions.

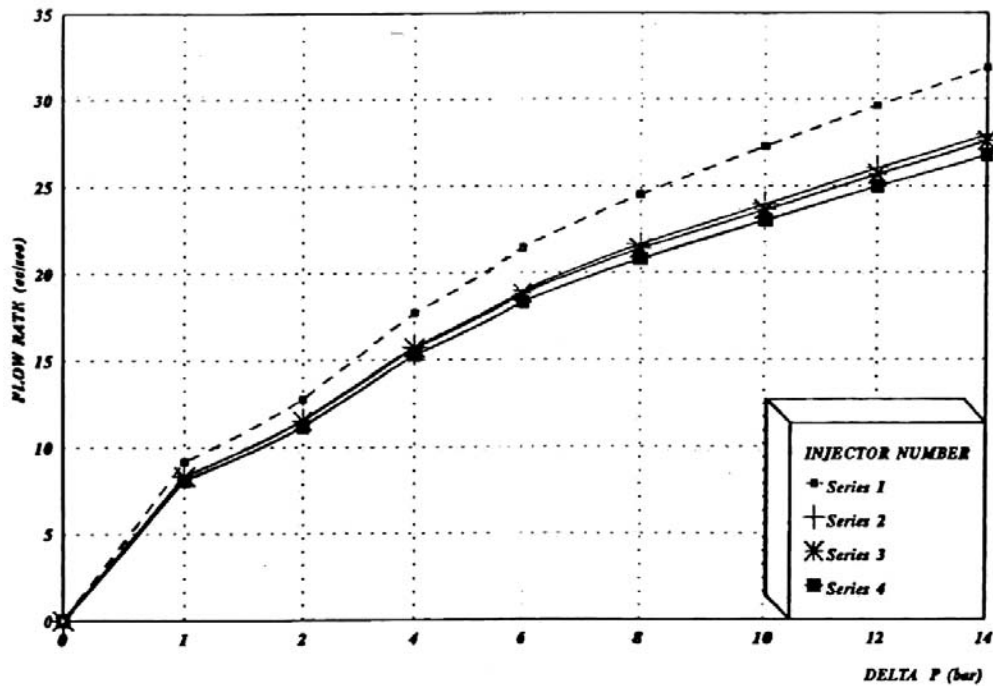


Fig.9 Changes in the discharge rate of inner injector versus pressure

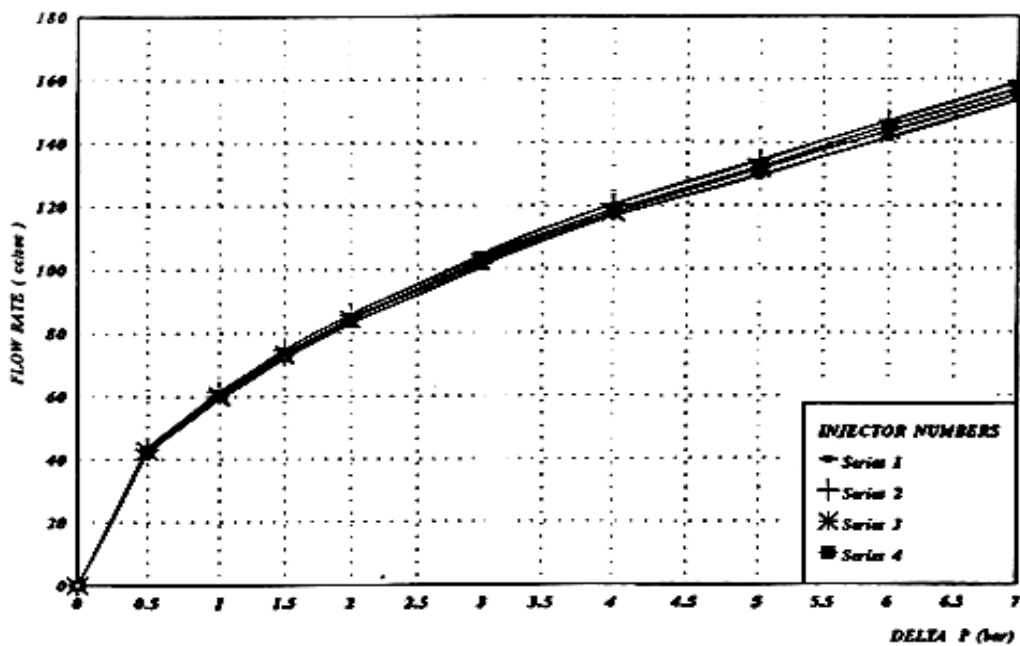


Fig. 10 Discharge rate of outer injector versus pressure

The experimental relation of maximum discharge rate is as the following:

$$\left(\frac{\Delta G}{G}\right)_{\max} = 1.33 \frac{\Delta d_c}{d_c} + 1.34 \frac{\Delta d_{Bx}}{d_{Bx}} + 0.67 \frac{\Delta R}{R} \quad (40)$$

Based on the production process precision, the maximum design error is around 16% which adds up to 26% with considering the design error. Fig. 9 shows the variation of inner injectors mass flow rate versus the pressure difference. The average discharge rate of 3 injectors in 10 bar pressure is 2356 cc/sec. Therefore, the discharge rate error will be 17.8%; however, this error has been predicted less than the maximum predicted error of 26%. By decreasing the design and production inaccuracy, one could decrease discharge rate error.

Fig.10 shows the variation of outer injectors discharge rate per pressure difference; that is 4 bars, is 118.5 cc/sec. Therefore, the error in the discharge rate is 18.5% and it is less than maximum error predicted; that is, 26%. The spray umbrella of these injectors in 0.16 bar pressure is changed from tulip shape to cone shape.

We performed another test to study the effect of existing an internal injector, particularly its nozzle on the discharge rate of external injector/ First, we made a part that could replace internal injector but lack its lower parts (nozzle) and this part was assembled in the external injector, instead of the internal injector. The external injector was then tested. According to this test, it was revealed that there would be not much variation in discharge rate; in another word, the existence of nozzle of internal injector would leave no effects on the path and movement of flux in outer injector.

6. CONCLUSION

A theoretical design procedure for double-base liquid-liquid centrifugal injectors is presented. A computer code is developed for the proposed method and the results are compared with experimental data. According to these comparisons one has to develop more precise manufacturing procedures in order to decrease the amount of errors.

REFERENCES

- [1] Ditiakin, E.F., Koliachko, L.F., Noikov, B.V., Yagodkin, V.E., "Fluids Spray", Moscow, 1977 .
- [2] Vasiliou, A.P., Koderaftsov, B.M., Korbatinkov, B.D., Ablintsky, A.M., Polyayov, B.M. Palvian, B.Y., "Principles of Theory and Calculations of Liquid Fuel Jet", Moscow, 1993.
- [3] Rammurthi, K., Tharakan, J., "Experimental Study of Liquid Sheets Formed in Coaxial Swirl Injectors", J. of Propulsion and Power, VOL. 11, No. 6, 1995.
- [4] Sivakumar, D., Raghunandan, B.N., "Jet Interaction in Liquid-Liquid Coaxial Injectors", J. of Fluid engineering, VOL. 118, June 1996.
- [5] Sutton, G. P., "Rocket Propulsion Elements", John Wiley & Sons, 1986, Fifth Ed.
- [6] Huzel, D.K., Huang, D.H., "Design of Liquid Propellant Rocket Engineering", Nasa, 1971, Second Ed.
- [7] Barrerf, M., "Rocket Propulsion", Paris, 1959.
- [8] Chuech, S.G., "Numerical Simulation of No swirling and Swirling Annular Liquid Jets", AIAA J., VOL 31, No. 6, June 1993.
- [9] Shames, E. Herman, "Mechanics of Fluids", 4th Printing 1988, McGraw-Hill.
- [10] Bazarov, V.G., Yang, V., "Liquid-Propellant Rocket Engine Injector Dynamics", J. of Propulsion and Power, VOL. 14, NO. 5, 1998.
- [11] Jeng, S.m., Jog, M.A., Benjamin M.A., "Computational and Experimental Study of Liquid Sheet Emanation from Simplex Fuel Nozzle", ALAA Journal, Vol. 36, No. 2, 1998.
- [12] Parlange, J.Y., "A Theory of Water-Bells ", J. of Fluid Mechanics, VOL. 29, Part 2, 1967 .
- [13] Ghafourian, A., Mahalingam, S., Dindi, H., Daily, J.W., "A Review of Atomization in Liquid Rocket Engines ", AIAA Paper 91-0283.
- [14] Sankar, S.V., Wang, G., Rudoff, R.C., Isakovic, A., Bachalo W.D., "Characterization of Coaxial Rocket Injector Sprays Under High Pressure Environments", ATTA Paper 1991.
- [15] Fischer, U., Valinejad, A., "Tables and Standards of Design and Machinery", Taban, Iran.